Electronic Supplementary Material (ESI) for Physical Chemistry Chemical Physics.

SUPPORTING INFORMATION

Local water sensing: Water exchange in bacterial photosynthetic reaction centers embedded in a trehalose glass studied by multiresonance EPR

A. Nalepa,[a] M. Malferrari[b], W. Lubitz[a], G. Venturoli[b,c], K. Möbius[a,d] and A. Savitsky[a]

[a] Max-Planck-Institut für Chemische Energiekonversion , Stiftstr. 34-36, D-45470 Mülheim (Ruhr), Germany

[b] Laboratorio di Biochimica e Biofisica, Dipartimento di Farmacia e Biotecnologie, FaBiT, Università di Bologna, via Irnerio 42, I-40126 Bologna, Italy.

[c] Consorzio Nazionale Interuniversitario per le Scienze Fisiche della Materia (CNISM), c/o Dipartimento di Fisica, Università di Bologna, via Irnerio 46, I-40126 Bologna, Italy.

[d] Department of Physics, Free University Berlin, Arnimallee 14, D-14195 Berlin, Germany.

Description of bRC photocycle

The photosynthetic reaction center (RC) from the purple bacterium *Rhodobacter (Rb.) sphaeroides* is a membrane-spanning pigment-protein complex which catalyses the primary photochemical events that initiate solar-energy conversion in the photosynthetic bacteria. Within the RC from *Rb. sphaeroides* (see Figure 1a main text), following photon absorption, the primary electron donor P_{865} (a bacteriochlorophyll *a* dimer) delivers an electron in ≈200 ps to the primary quinone acceptor Q_A (a ubiquinone-10), located ≈25 Å away from P_{865}, thus generating the primary charge-separated state $P_{865}^{\bullet+}Q_A^{\bullet-}$ (for reviews, see refs.[1,2]). From $Q_A^{\bullet-}$ the electron is then transferred, in a conformationally gated process, to a secondary quinone molecule Q_B (also a ubiquinone-10), acting as a two-electron, two-proton acceptor upon successive photochemical turnovers of the RC.[3] The different redox properties of Q_A and Q_B, in spite of being chemically identical ubiquinone-10 molecules, are rooted in the different micro-environment of their protein binding sites: Q_A accepts only one electron and is not protonated, whereas Q_B sequentially accepts two electrons and two protons to form the dihydroquinone Q_BH_2 [4]. When electron donors to $P_{865}^{\bullet+}$ are not available, in Q_B-deprived RCs (or in the presence of inhibitors of the $Q_A^{\bullet-}$-to-Q_B electron transfer) the RC returns to its ground state by direct electron tunnelling[5] from $Q_A^{\bullet-}$ to $P_{865}^{\bullet+}$ (primary charge recombination).

Transient EPR signals in Zn-bRC

In the dark-adapted state of the Zn-bRC variant, a residual echo-detected EPR signal from $Q_A^{\bullet-}$ is present, see Fig. S1. The $P_{865}^{\bullet+}Q_A^{\bullet-}$ radical-pair state was generated in Zn-bRCs by continuous light illumination, resulting in a steady-state EPR signal. When the diode laser was switched off, the EPR signal of the radical-pair state decays and virtually no accumulated $P_{865}^{\bullet+}$ signal is observed, see Fig. S1. Hence, there is no irreversible photo-damage to the bRCs during continuous sample illumination.

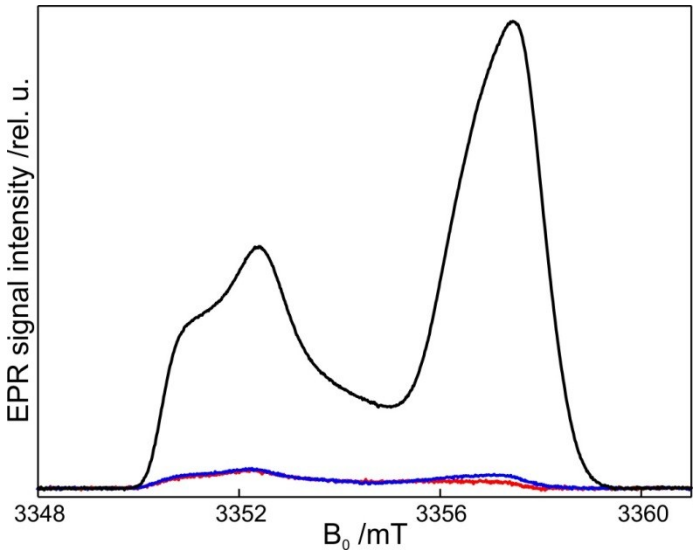

Figure S1. Field-swept echo detected W-band EPR spectra of dark-adapted Zn-RCs in trehalose (r =11%) at 130 K prior to illumination at 690 nm (red trace), under continuous illumination at 690 nm (black trace), and after the 690 nm diode laser is switched off (blue trace).

Details of W-band EDNMR experiments

For the detection of D nuclei in R1/trehalose and SL-bRC/trehalose, the HTA pulse length was set to 14 μs at $\omega_1^{HTA}(\nu_1)/2\pi$ = 3.7 MHz mw field amplitude. The echo integration window was set to 1.2 μs. For the detection of D nuclei in Zn-bRC, due to the overlap with the ^{14}N signal, the mw field amplitude was decreased to 2.7 MHz and the HTA pulse length increased to 16 μs. The echo integration window was set to 600 ns. For the detection of ^{14}N nuclei in R1/trehalose, the HTA pulse length was set to 1.1 μs at $\omega_1^{HTA}(\nu_1)/2\pi$ =6 MHz mw field amplitude. The echo integration window was set to 1.0 μs. For the detection of ^{17}O nuclei in SL-bRC/trehalose, the HTA pulse length was set to 20 μs at 2.6 MHz mw field amplitude. The echo integration window was set to 800 ns. The length of the π/2 pulse in the detection sequence was always set to 100 ns, the inter-pulse separation was adjusted depending on the chosen integration window. The detection sequence was usually set to 4 μs after the HTA pulse in order to ensure the decay of electron-spin coherency.

Evaluation of EDNMR spectra

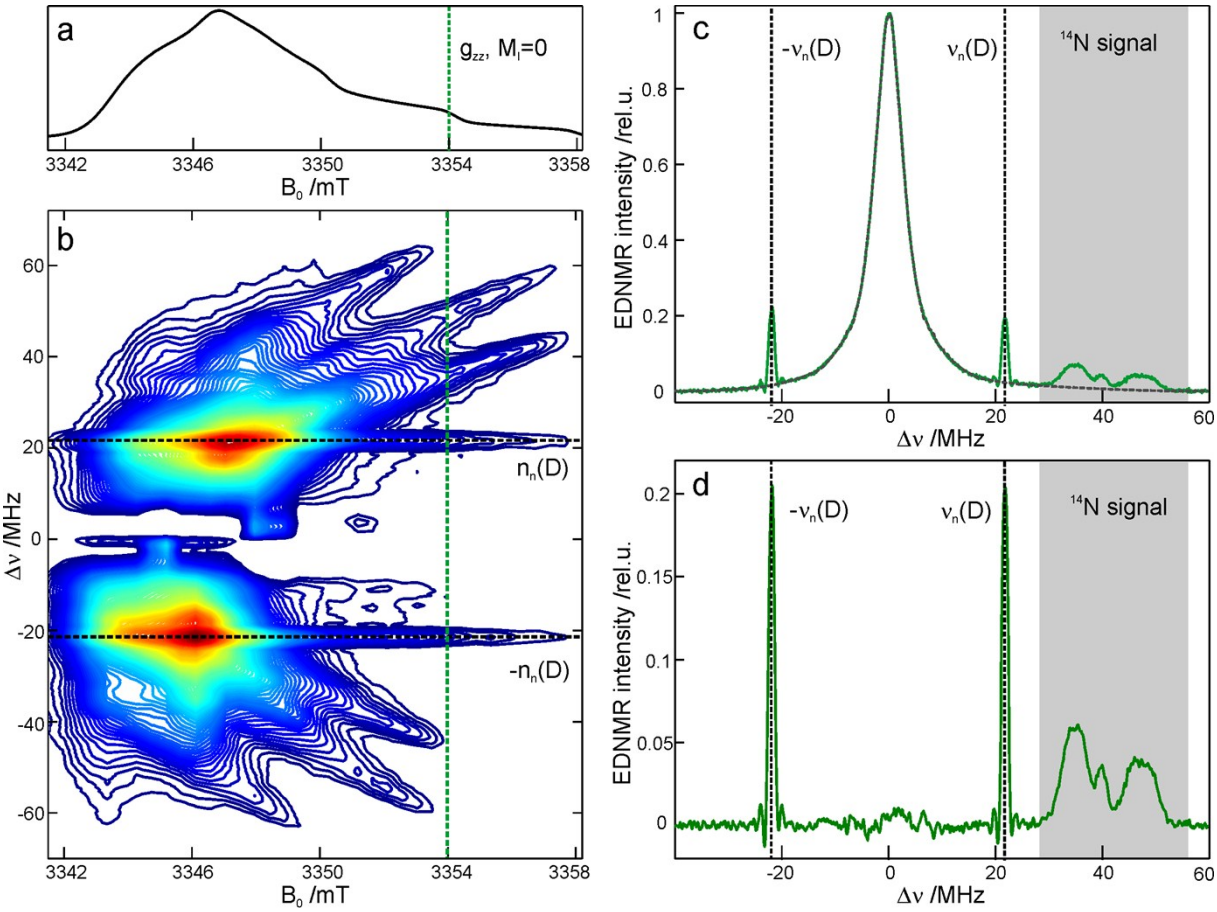

Figure S2. (a) W-band two-pulse echo-detected field-swept EPR spectrum for R1 nitroxide embedded in trehalose glass at $r = 74\%$ ($NaCl/D_2O$). (b) Contour plot of the frequency-field dependence of the EDNMR signals acquired for R1 in trehalose glass equilibrated at $r = 74\%$ (D_2O). The spectra were recorded at 60 K. (c) W-band EDNMR spectrum recorded at g_{zz}, M_I=0 spectral field position. The spectrum was inverted and normalized. The signal at the deuterium Larmor frequency at the right and left hand side of spectrum is marked with a dashed line. The signals due to internal ^{14}N are marked with a grey rectangle. The fit of the Lorentzian line to the central blind spot is shown by the black dashed line. (d) EDNMR spectrum in (c) after blind spot subtraction. The difference in D line intensity is mostly due to the cavity profile. The reported intensity of the deuterium line is the average of intensities for both line at $\Delta\nu>0$ and at $\Delta\nu<0$.

EDNMR D-line intensities during $LiCl/D_2O$ sample equilibration

Table S1. The intensity of the D-line EDNMR for SL-RC embedded in the trehalose glass equilibrated at r = 11% ($LiCl/D_2O$).

Equilibration time /h	D-line EDNMR intensity
3	0.0080± 0.0005
6	0.0100± 0.0005
16	0.030± 0.001
27	0.043± 0.001
50	0.070± 0.004
70	0.070± 0.005
170	0.066± 0.004
70 (prepared in D_2O)	0.155± 0.005

EDNMR ^{14}N-line intensities during $NaCl/D_2O$ sample rehydration

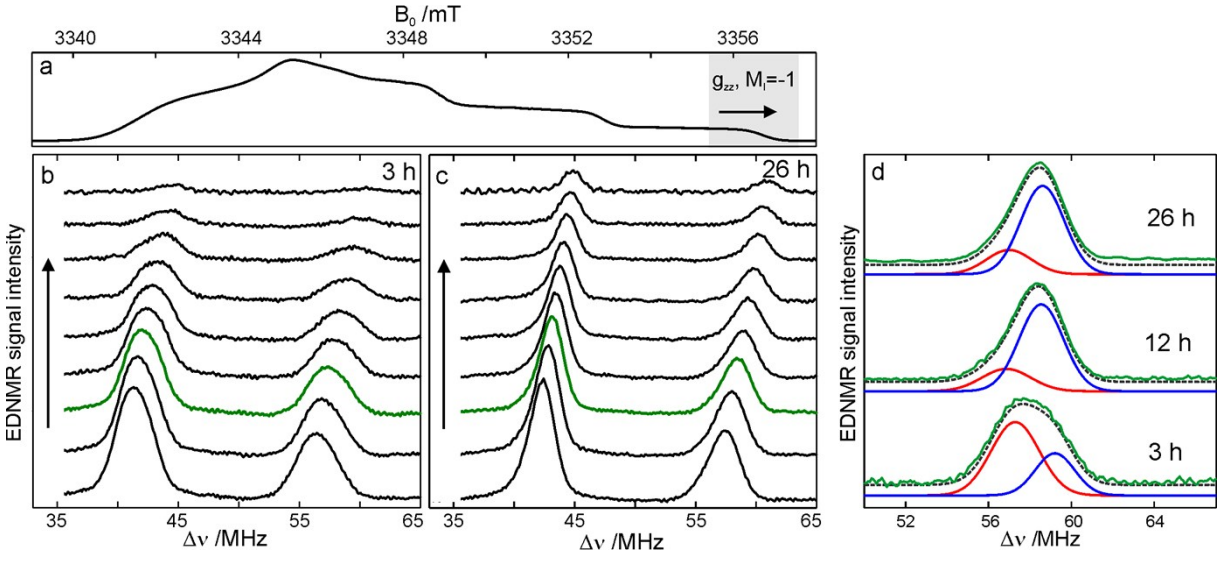

Figure S3. W-band EDNMR spectra in g_{zz}, M_I=-1 spectral region for R1/trehalose glasses rehydrated at r = 74% for 3h (b) and 26 hours (c). (d) W-band EDNMR spectra recorded close to g_{zz}, M_I=-1 spectral field position in the frequency range corresponding to the high frequency ^{14}N EDNMR line. The R1/trehalose glasses were rehydrated for 3, 12 or 26 hours. The two Gaussian lines show contributions to the ^{14}N signal stemming from single (red line) and double (blue line) hydrogen bonded R1 fractions to the ^{14}N signal, for more information see [6].

Table S2. The magnetic parameters of the single (1) and double (2) hydrogen bonded R1 in trehalose glasses equilibrated at r = 74% for the indicated period of time obtained from the analysis of W-band EDNMR recordings in the g_{zz}, M_I=-1 spectral region.

	R1/trehalose glass after 3 hours	R1/trehalose glass after 26 hours
$\Delta\nu^1_{1/2}$ /MHz	2.7±0.2	2.6±0.2
$\lvert A^1_{zz}\rvert$ /MHz	100.8±0.3	101.1±0.3
fraction of 1	0.68±0.05	0.22±0.05
$\Delta\nu^2_{1/2}$ /MHz	2.2±0.2	2.5±0.2
$\lvert A^2_{zz}\rvert$ /MHz	105.6±0.3	105.6±0.3
fraction of 2	0.32±0.05	0.78±0.05

EDNMR D-line during NaCl/D_2O sample rehydration

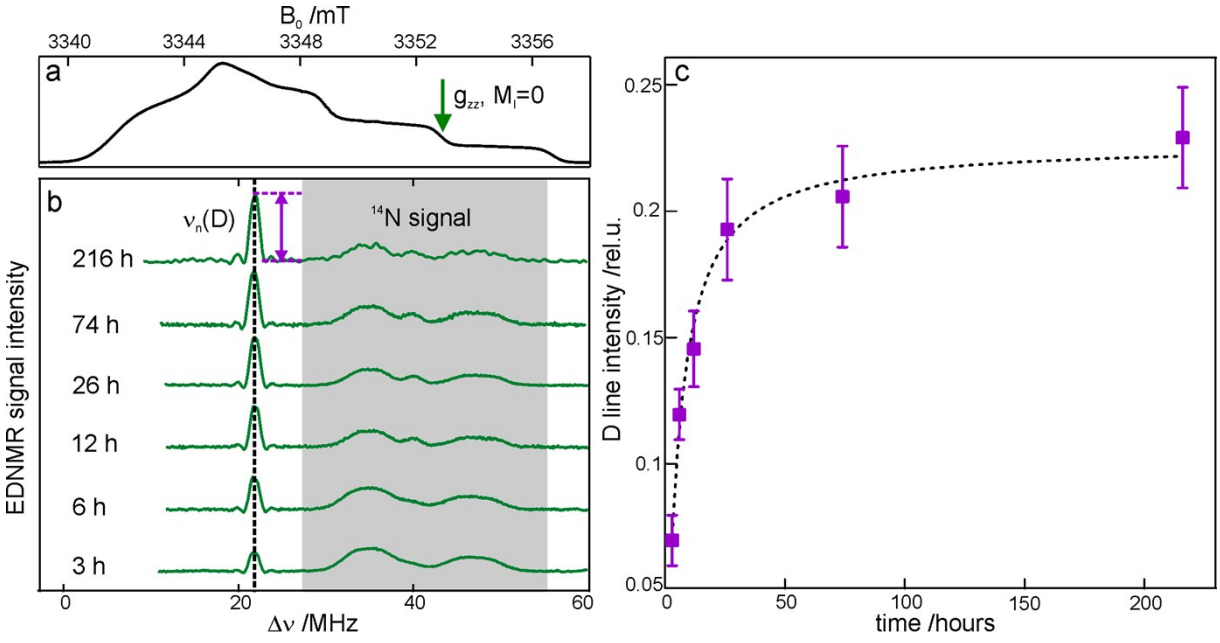

Figure S4. (a) Echo-detected field-swept EPR spectrum of nitroxide radical R1 embedded in trehalose glass. The g_{zz}, M_I=0 spectral position is marked. (b) EDNMR spectra recorded for R1 /trehalose glassess rehydrated for the indicated amount of time at r = 74% (NaCl/D_2O). The spectra were recorded at the field position indicated by a green arrow in (a). (c) The intensity of the deuterium EDNMR line as a function of equilibration time.

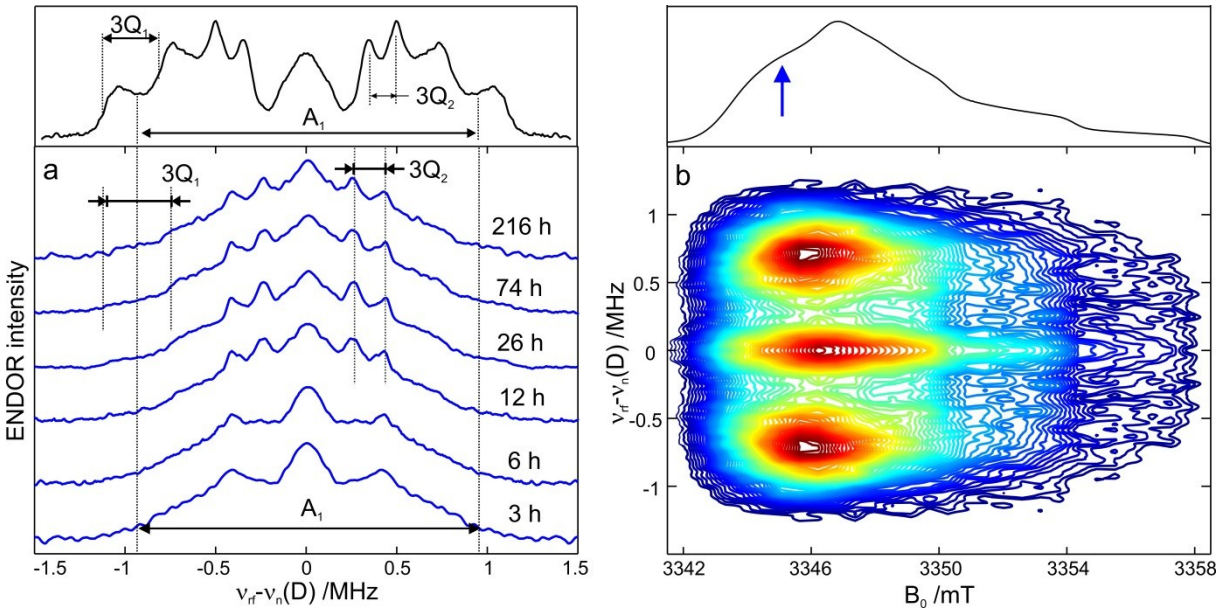

Figure S5. (a) W-band Mims ENDOR spectra recorded for R1/trehalose glasses equilibrated for different amount of time at r = 74% ($NaCl/D_2O$). The spectra were recorded at the field position marked by the blue arrow in (b). The quadrupole and hyperfine splittings are assigned according to the reference measurement of R1 in frozen CH_3OD solution shown on the top. (b) W-band D Mims ENDOR recordings taken at field positions across the R1 spectrum shown on top for R1/trehalose glass equilibrated at r = 74%. The separation between the first two π/2 pulses in the pulse sequence was set to τ=250ns (a) or 320ns (b) and t_{rf}=35 μs. The contour lines are shown as isohypses from 0.05 to 1 of the maximum ENDOR intensity. The spectra were recorded at 60 K. On top the echo-detected EPR spectrum is shown.

Deuterium ENDOR on Zn-bRC after NaCl/D_2O sample rehydration

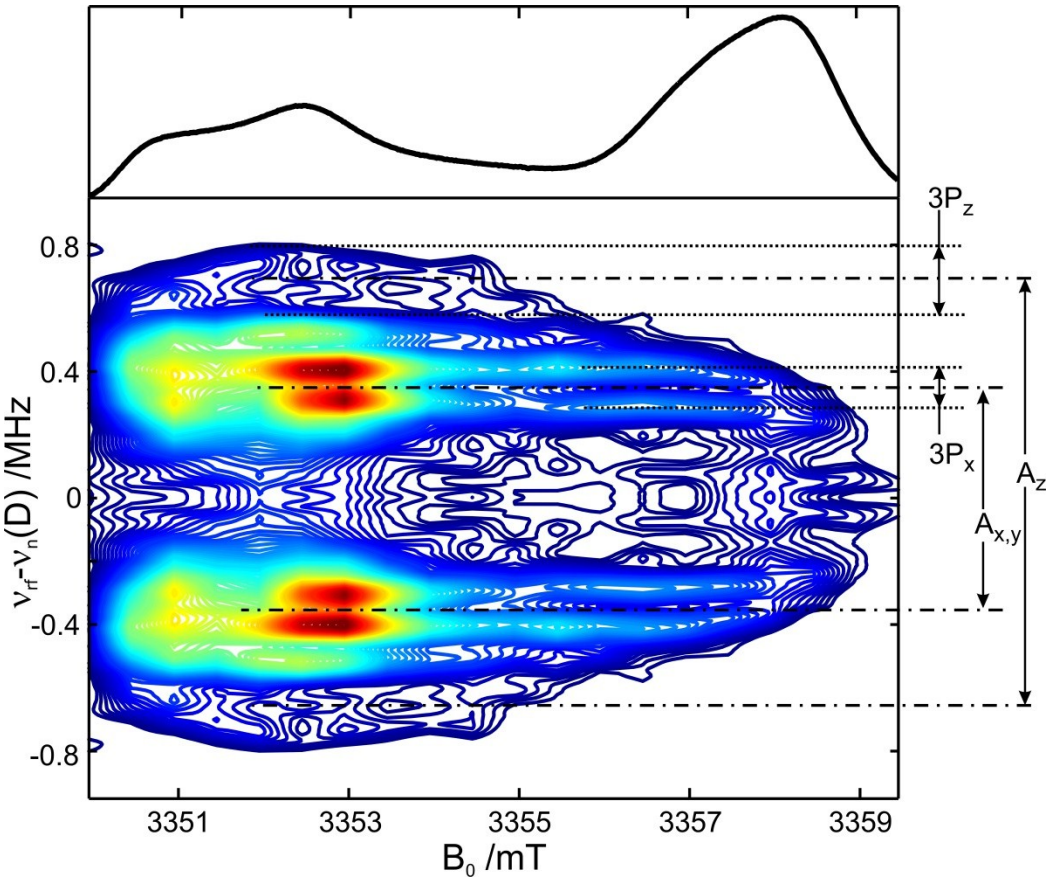

Figure S6. W-band D Mims spectrum spectra for Zn-bRC in trehalose glass equilibrated at $r = 74\%$ ($NaCl/D_2O$). The spectra were recorded at 130 K under continuous illumination at 690 nm. The separation between the first two π/2 pulses in the pulse sequence was set to τ=360 ns and t_{rf}= 35 µs. On top the echo-detected EPR spectrum is shown. The orientation dependence of hyperfine and quadrupole ENDOR responses is in good agreement with results reported previously [7].

Table S3. Comparison of magnetic parameters obtained from analysis of deuterium ENDOR spectra of Zn-bRC embedded in trehalose rehydrated at $r = 74\%$ (D_2O) with previously published parameters obtained for Zn-bRC dissolved in D_2O [7].

	A_x' /MHz	**A_y' /MHz**	**A_z' /MHz**
N-D·····O_4 (His M219)	-0.98±0.01	-1.00±0.01	+1.36±0.02
N-D·····O_1 (Ala M260)	-0.70±0.01	-0.76±0.01	+1.37±0.03
this work	-0.69±0.05	-0.72±0.05	+1.35±0.05
	P_x'' /kHz	**P_y'' /kHz**	**P_z'' /kHz**
N-D·····O_1 (Ala M260)	-70±6	-31±8	+101±10
this work	-44±0.01	-30±0.01	+72±10

1. G. A. Feher, J.P.; Okamura, M.Y.; Rees, D.C. , *Nature*, 1989, **33**, 111.
2. A. J. Hoff and J. Deisenhofer, *Physics Reports-Review Section of Physics Letters*, 1997, **287**, 2-247.
3. M. Y. Okamura, M. L. Paddock, M. S. Graige and G. Feher, *Biochim Biophys Acta*, 2000, **1458**, 148-163.
4. J. Koepke, E. M. Krammer, A. R. Klingen, P. Sebban, G. M. Ullmann and G. Fritzsch, *Journal of Molecular Biology*, 2007, **371**, 396-409.
5. J. D. McElroy, D. C. Mauzerall and G. Feher, *Biochim Biophys Acta*, 1974, **333**, 261-278.
6. P. Gast, R. T. L. Herbonnet, J. Klare, A. Nalepa, C. Rickert, D. Stellinga, L. Urban, K. Möbius, A. Savitsky, H. J. Steinhoff and E. J. J. Groenen, *Phys. Chem. Chem. Phys.*, 2014, **16**, 15910-15916.
7. M. Flores, R. Isaacson, E. Abresch, R. Calvo, W. Lubitz and G. Feher, *Biophys. J.*, 2007, **92**, 671-682.